

## Porosity and the Effect of Structural Changes on the Mechanical Glass Transition Temperature

STEFAN KASAPIS\*

Department of Chemistry, National University of Singapore, Block S8, Level 5, Science Drive 3,  
 Singapore 117543

SHYAM S. SABLANI, M. SHAFIUR RAHMAN, AND INSAF M. AL-MARHOABI

Department of Food Science & Nutrition, College of Agricultural & Marine Sciences,  
 Sultan Qaboos University, P.O. Box 34, Al-Khod 123, Oman

ISSA S. AL-AMRI

Department of Pathology, College of Medicine & Health Sciences, Sultan Qaboos University,  
 P.O. Box 34, Al-Khod 123, Oman

---

Continuing an investigation on the fundamentals and applications of a recently proposed concept, i.e., the mechanical or network glass transition temperature, we now report data on the macrostructural changes in dehydrated apple tissue in relation to apparent porosity. Care was taken to keep the moisture content of the matrix constant ( $\approx 81\%$ ) while the volume fraction of total pores ranged from 0.38 to 0.79. Reproducible mechanical profiles identified the first derivative of shear storage modulus as a function of temperature to be the appropriate indicator of the mechanical  $T_g$  at the conjunction of the William–Landel–Ferry/free volume theory and the modified Arrhenius equation. Information on the microstructural characteristics and morphology of porous apple preparations was also made available via modulated differential scanning calorimetry and scanning electron microscopy. The work reveals and discusses discrepancies in the  $T_g$ –porosity relationship obtained from calorimetry and mechanical analysis attributable to the different extent to which the two techniques respond to degrees of molecular mobility.

---

**KEYWORDS:** Dried apple tissue; porosity; thermomechanical analysis; mechanical glass transition temperature

### INTRODUCTION

In the last 80 years or so, studies have documented that organic materials subjected to rapid cooling possess temperature ranges in which they may change to “vitreous solids” or “glasses” (1). These are formed when the system is cooled so rapidly that there is no time for the molecules to rearrange themselves and pack into crystalline domains. In the “glassy state”, characteristics exhibited are those of brittleness, high strength, clarity, and ultimately low molecular mobility in the “supercooled liquid” (2). Upon heating, materials soften progressively and macromolecular matrices achieve properties related to the “rubbery state”. Examples of partial/total glassy behavior include hair, dry cotton shirts, biscuits, coffee granules, pasta, spaghetti, and ice cream as well as inorganic oxide systems, organic/inorganic polymers, and carbohydrate or

protein matrices in aqueous environment or in mixture with high levels of sugars (3).

In foods, the glass phenomenon has been introduced rather recently following appreciation by the food-processing industry of the inadequacy of the water–activity concept as a universal standard of quality control (4). Earlier, the importance of the glassy state was highlighted by White and Cakebread (5). They discussed the importance of the glassy and rubbery states in relation to the quality control of a number of high solids systems. Vitrification was considered as a reference point for the development of a new branch of technology, and generally, discussion of properties has been in terms of temperatures above or below the glass transition temperature,  $T_g$  (6–8). Thus, a low  $T_g$  means that at room temperature the food is soft and relatively elastic, and at higher temperatures, it may even flow. In contrast, a food with a high  $T_g$  will be hard and brittle at ambient temperature.

Traditionally, differential scanning calorimetry (DSC) has been used to measure vitrification processes by providing a

---

\* To whom correspondence should be addressed. Tel: (65)6516 4834. Fax: (65)6775 7895. E-mail: chmsk@nus.edu.sg.

direct, continuous measurement of a sample's heat capacity (9, 10). Clearly, water plasticizes food materials and DSC has been used widely to estimate the  $T_g$  values for sugars, oligosaccharides, proteins, maltodextrins, and starches at various levels of water content (11, 12). This greatly advanced the concept of a "state diagram", which is useful in evaluating the effects of food composition on glass transition-related properties that affect the shelf life and quality (13, 14). In parallel with thermal studies, mechanical measurements have been employed, and recently, the concept of network or mechanical  $T_g$  was proposed (15). This aims to be an index of physical significance that relates to a threshold of the free volume theory in the glass transition region and the reaction rate theory in the glassy state.

It has been demonstrated that the glass transition temperature measured by calorimetry remains unaltered by the presence of low levels of polysaccharide (0.5–3%) in a high sugar environment (70–93%) suggesting that the mobility of the sugar is unaffected by the presence of the macromolecule (16). However, the mechanical profile of the rubber-to-glass transition is strongly influenced by the polysaccharide particularly if it is network forming. Applications of the network  $T_g$  were explored in model confections, dried fish muscle and fruit leathers, state diagrams, and adsorption isotherms (17). We also felt that pore formation, which affects irreversibly cellular structure during dehydration (18–20), should be reflected in mechanical measurements. Therefore, changes in structural properties due to porosity may relate to the mechanical glass transition temperature, and the present communication offers insights into this under-researched area.

## EXPERIMENTAL PROCEDURES

**Material Preparation.** Fresh apples (French Royal Gala) were purchased from a local grocery in Muscat, Oman, and stored at refrigeration temperature (3–4 °C) for 24 h. Then, the apples were peeled and cylindrical disks (2.5 cm diameter; 1.0 cm height) were prepared using a stainless steel corer and a sharp knife. The moisture content was measured gravimetrically by drying the disks in a vacuum oven at 70 °C for at least 24 h. Thus, the moisture content of the fresh tissue was found to be  $88.48 \pm 0.63\%$  (standard deviation). Drying affects the pore characteristics in the final product, and distinct protocols (air, vacuum, and freeze drying) were utilized in our study to maximize the experimental range of porosities (21). Thus, air drying was carried out at 50 or 70 °C between 7 and 8 h; vacuum drying was carried out at a chamber temperature and pressure of 50 °C and 25 kPa for 8 h; and freeze drying was carried out at 100 Pa and a constant shelf temperature of –20 °C for 24 h, with the cylindrical samples being stored at –40 °C for at least 48 h prior to placement in the freeze dryer.

Different drying techniques produced materials with a varied level of porosity and moisture content. Following dehydration, the moisture content of the apple samples was 4–7%. Because the concept of water plasticization and its effect on the glass transition temperature may obscure the effect of porosity on the same, all materials were brought to a nearly identical moisture content. Thus, they were stored in air-sealed glass jars that had reached low-equilibrium relative humidity with a saturated salt solution of potassium acetate. The low relative humidity system ( $\approx 22\%$ ) allowed uniform and gentle moisture transfer within the confined environment of the glass jars (22). The total number of dehydrated samples that were equilibrated was 42. In doing so, they were removed periodically and weighted until the mass reached a constant value ( $\pm 0.001$  g), as read on an electronic balance. The moisture content of the final products for each apple porosity sample was  $19 \pm 0.5\%$ . Selected final products were also analyzed for water activity, which ranged randomly between 0.73 and 0.77.

**Porosity Measurements.** To accommodate slight changes in the structure of apples due to absorption/desorption of water during the equilibration process, porosity values were determined following this

final stage. The volume fraction of voids in the sample was considered to be a good measure of the apparent porosity ( $\epsilon_a$ ), which is calculated as:

$$\epsilon_a = 1 - \frac{\rho_a}{\rho_s} \quad (1)$$

where  $\rho_a$  and  $\rho_s$  are the apparent and substance densities, respectively (23). Apparent density values of the equilibrated tissue were estimated from the "buoyant force method" (3). Preweighted samples were coated with a thin layer of paraffin wax, and the buoyant force of the coated disk was recorded by measuring the mass in air and water. Wax coating prevented exchange of material from/to the sample, and a sinker was used to avoid its partial floating.

The substance density of the material at any moisture content can be measured using the following mathematical expression, which assumes conservation of mass and volume within the multicomponent matrix (24):

$$\frac{1}{\rho_s} = \frac{X_w}{\rho_w} + \frac{X_s}{\rho_s^0} \quad (2)$$

where  $\rho_w$  is the density of water (995 kg/m<sup>3</sup> at 23 °C),  $\rho_s^0$  is the density of unhydrated ground apple powder (1621 kg/m<sup>3</sup>) (25), and  $X_w/X_s$  are the mass fractions of water and solids, respectively.

**Small Deformation Dynamic Oscillation.** Tests were performed using the Advanced Rheometrics Expansion System (ARES), which is a controlled strain rheometer (Rheometric Scientific, Piscataway, NJ). The ARES had an air-lubricated and essentially noncompliant force rebalance transducer with a torque range between 0.02 and 2000 g cm. This facilitated accurate recording of the rigidity of materials with a glassy consistency. For precise control of sample temperature, an air convection oven was used, which had a dual element heater/cooler with counter-rotating air flow covering a wide temperature range. The experimentally accessible temperature allowed recording of the viscoelastic properties of dried apple deep into the glassy state. In doing so, the parallel-plate geometry was preferred, with the diameter of the top plate being 8.0 mm. The measuring gap between the plates was fixed at 3 mm.

Samples in the form of cylindrical disks were loaded on the plate of the rheometer at ambient temperature, cooled to –70 °C, and then heated back at a scan rate of 1 °C/min. During the temperature runs, they were subjected to an oscillation on shear of set frequency (1 rad/s) and strain that varied from 2% in the rubbery plateau to 0.00075% in the glassy state (26). To minimize changes in the moisture content due to the low vapor-pressure environment in the oven, exposed edges of the apple tissue were covered with a silicone fluid from BDH (100 cs). Two replicates were analyzed for each experimental apparent porosity, with the rubber-to-glass transition being readily reproducible within a 3% error margin as a function of temperature or time scale of measurement.

**Modulated DSC.** Measurements were taken on a TA Instruments Calorimeter Q1000 with autosampler (TA Instruments Ltd., Leatherhead, United Kingdom). The instrument used a refrigerated cooling system to achieve temperatures of –90 °C and a nitrogen DSC cell purge at 25 mL/min. Hermetic aluminum pans of 30  $\mu$ L capacity were used. Temperature and heat flow of the instrument were calibrated using a traceable indium standard (mp 156.5 °C;  $\Delta H_m = 28.3$  J/g) and distilled water (mp 0 °C;  $\Delta H_m = 334$  J/g), and the heat capacity response using a sapphire standard. Small size samples of 7–10 mg were cut from the dried apple tissue using a sharp knife. Great care was taken to avoid any compression of the cylindrical disks while cutting, thus preventing distortion of the original porosity profile. Preparations were cooled at rate of 1 °C/min to –90 °C and left there for 30 min, and the glass transition was determined from the midpoint of the heat capacity change observed at the same heating rate. Samples were analyzed at  $\pm 0.53$  °C temperature amplitude of modulation and 40 s period of modulation (27). The reference was an empty hermetically sealed aluminum DSC pan. Three runs were generally taken, and the average

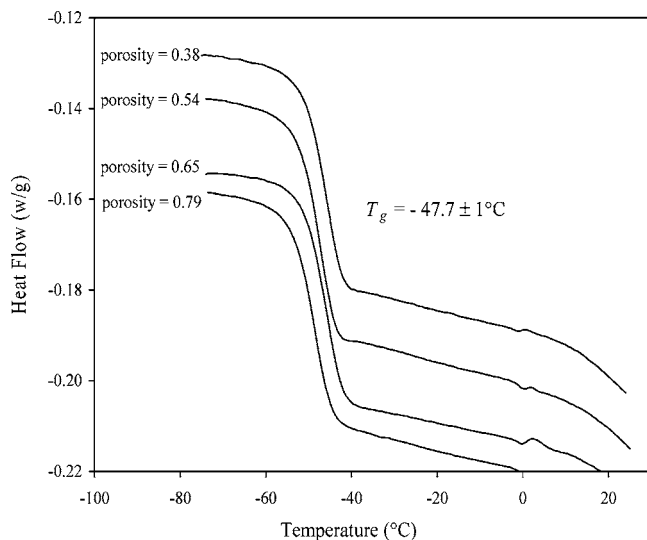


**Figure 1.** Heat flow variation as a function of temperature for dehydrated apple tissue with a solid content of  $\approx 81\%$  obtained with MDSC at a heating rate of  $1\text{ }^\circ\text{C}/\text{min}$ . Values of apparent porosity are shown to the left of the individual traces.

of essentially overlapping traces was considered as the glass transition at subzero temperatures.

**Scanning Electron Microscopy.** Dried apple specimens were fragmented under a stereomicroscope to small sizes of  $0.3\text{ cm}$  using a razor blade and placed in Karnovsky's fixative (2% glutaraldehyde and 4% paraformaldehyde containing  $1\text{ M}$  cacodylate buffer) for  $2\text{ h}$  at  $4\text{ }^\circ\text{C}$  (28). Following fixation, the apple fragments were washed in three  $10\text{ min}$  changes of  $1\text{ M}$  cacodylate buffer. Secondary fixation was carried out in  $1\%$  osmium tetroxide in distilled water for  $60\text{ min}$ . Three additional  $10\text{ min}$  changes in distilled water were carried out to wash off excess osmium tetroxide. The samples were placed in graded concentrations of acetone (25, 50, 75, and 90%) for  $10\text{ min}$ , and this was followed by three changes of absolute acetone, two of which were for  $15\text{ min}$  and the third one for  $60\text{ min}$ , thus ensuring complete removal of water. The apple specimens were then dried and adhered to  $10\text{ mm}$  silver stubs coated with carbon discs under a stereomicroscope to expose the different sides of the specimens for examination. Stubs of specimens were sputter coated with gold particles for  $135\text{ s}$  using Bio-Rad SEM Coating System in order to provide a reflective surface for the electron beam. These were examined with a scanning electron microscope operated at  $10\text{ kV}$  (Jeol JSM-5600LV; Japan Electron Optics Ltd., Tokyo, Japan). Topographic images of the ultrastructure of apple porosity were recorded and saved.

## RESULTS AND DISCUSSION

**First Observations on Porosity and the Glass Transition Temperature Using Thermal Analysis.** Thermal analysis is being used increasingly to elucidate the molecular mechanisms involved in various relaxations including temperatures of the glass transitions. Empirical data from DSC were sought in this part of the work as a first indication of the effect of porosity on the state transition of the dehydrated apple tissue. The composite diagram of heat flow curves for apple with an extensive range of apparent porosities (from  $0.38$  to  $0.79$ ) is shown in **Figure 1**. Samples were cooled slowly ( $1\text{ }^\circ\text{C}/\text{min}$ ) from ambient temperature ( $23\text{ }^\circ\text{C}$ ) and then heated at the same scan rate from temperatures well below the glass transition temperature of the mixture, thus exhibiting a "pseudo-equilibrium" relaxation response to the changing thermal regime. Furthermore, instrumental amplification and sensitivity settings are identical, sample weights are similar, and therefore, results are comparable.

In each case, the heat flow curve begins at the top (endothermic down), and this sigmoidal change is construed as

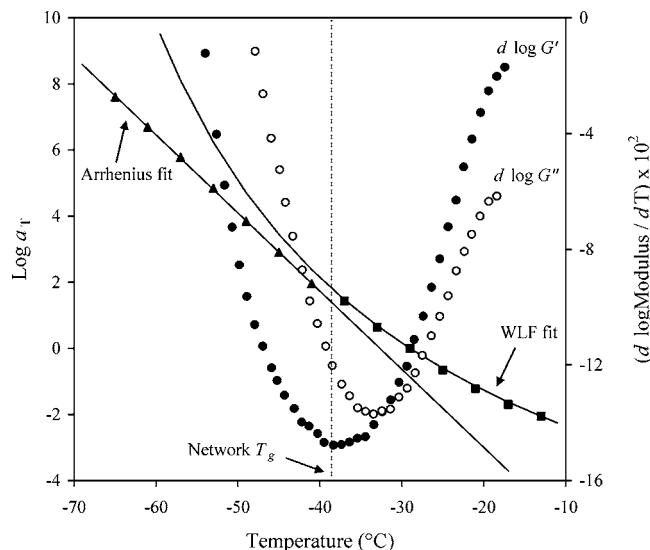


**Figure 2.** Temperature variation of the factor  $a_T$  within the glass transition region (■) and the glassy state (▲) for a mixture of  $2.33\%$   $\kappa$ -carrageenan with  $35.34\%$  glucose syrup plus  $35.33\%$  sucrose ( $25\text{ mM}$  KCl added), with the solid lines reflecting the WLF and modified Arrhenius fits of the shift factors in the glass transition region and the glassy state, respectively (left y-axis); first derivative plot of  $\log G'$  (●) and  $\log G''$  (○) as a function of sample temperature, with the dashed line pinpointing the prediction of the network  $T_g$  (right y-axis). Reprinted with permission from ref 17. Copyright 2006 Elsevier.

evidence of vitrification phenomena. The midpoint of this thermal event is readily detectable and is considered presently as the empirical glass transition temperature obtained from the MDSC thermogram. Often, this is referred to as  $T_{g2}$  in the literature, with researchers also reporting values for the beginning ( $T_{g1}$ ) and completion ( $T_{g3}$ ) of the heat capacity curve (29). Results of the present investigation argue strongly that there is no effect of porosity on the glass transition temperature of the thermal tests, which remains close to  $-47.7\text{ }^\circ\text{C}$  (**Figure 1**). Thus, the polymeric component of the apple tissue contributes to moderately higher DSC  $T_g$  values than for the simple preparations of monomeric polyhydric compounds reported in the literature (6, 30). The latter have been found to be about  $-55$  and  $-52\text{ }^\circ\text{C}$  from the state diagrams of glucose and fructose, respectively, at the same level of solids (81%).

**Concept of Mechanical or Network Glass Transition Temperature.** Elucidation of the possible effects of porosity on mechanical properties requires consideration of the macromolecular nature of the phenomenon of glass transition. This has been demonstrated first using the "synthetic polymer approach" for the vitrification of a sample of polyisobutylene rubber. Thus, the time and/or temperature dependence of rheological functions was found to follow the predictions of the Williams, Landel, and Ferry (WLF) equation, which acquired physical significance via the theory of free volume (31). In biomaterials, the combined WLF/free volume framework was utilized in preparations that find application in confections comprising, for example, a mixture of  $2.33\%$   $\kappa$ -carrageenan with  $35.34\%$  glucose syrup plus  $35.33\%$  sucrose ( $25\text{ mM}$  KCl added), and the outcome is reproduced in **Figure 2** (17).

The approach involves recording under shear frequency sweeps of storage modulus ( $G'$ ) and loss modulus ( $G''$ ) at temperature intervals of  $3\text{--}5^\circ$  and then superposing the modulus traces horizontally along the abscissa at an arbitrary chosen reference temperature ( $T_0$ ) within the glass transition region. This creates master curves of viscoelasticity of the reduced

variables,  $G_p'$  and  $G_p''$ , which are plotted in double logarithmic plots against the frequency of oscillation (32). Thus, mechanical functions, measured at the frequency range of 0.1–100 rad  $s^{-1}$  at a given experimental temperature  $T$ , are equivalent to those measured as the product of this frequency range times a scaling factor  $a_T$  (the so-called “shift factor”) at the reference temperature  $T_0$ . **Figure 2** illustrates the progression of shift factors taken at 14 different temperatures between  $-10$  and  $-70$  °C. Clearly, there is a change of pace in the logarithmic development of factor  $a_T$  as a function of temperature, which occurs at about  $-39$  °C.

The above outcome demarcates a passage from the glass transition region to the glassy state in the master curve of viscoelasticity, and it has been considered as the network  $T_g$  of the  $\kappa$ -carrageenan/cosolute mixture. This recent derivation of the glass transition temperature claims a theoretical advantage over the empirical indices of pictorial rheology reported earlier (33), since it stands at the blending of two distinct molecular processes. The WLF equation provides a good fit of the experimental shift factors in the glass transition region, thus making free volume the overriding mechanism behind molecular mobility (**Figure 2**). However, progress of the mechanical properties in the glassy state ( $<-39$  °C) is better described by the modified Arrhenius equation, which utilizes a set of experimental temperatures ( $T$ ) and the reference temperature (4). Unlike the WLF framework, parameterization through the reaction rate theory yields the concept of activation energy ( $E_a$ ) for an elementary flow process that is independent of temperature. In the following sections, the basic approach will be extended to dehydrated apple tissue in order to recognize the relationship between the volume fraction of total pores and structural/vitrification properties.

**Qualitative Observations of the Mechanical Vitrification of the Dehydrated Apple Tissue.** In rheological investigations of vitrification phenomena, one is faced with the fact that the effect of temperature variation at a controlled scan rate on the structural properties of dried foodstuffs (e.g., fruit leathers or fish muscle) is less pronounced than for model confections (typically polysaccharide or gelatin plus sugar), thus yielding a partial glass transition region in terms of temperature band and viscoelastic functions. Polysaccharide or gelatin systems in the presence of cosolute (sugar) exhibit classic viscoelastic vitrification, as reported in the synthetic polymer research (16, 32). Main features of the process include a dominant viscous component ( $G'' > G'$ ) within the confines of the glass transition region and a spectacular dependence of the mechanical functions on time or temperature that can be four or five orders of magnitude (from about  $10^5$  to  $10^9$  Pa). As shown in **Figure 3a–g**, however, the mechanical transition of typical dehydrated apple samples that have been cooled or heated at a rate of 1 °C/min is not that clearly defined.

To start with, the magnitude of the “rubbery” region is unusually high, with values being close to  $10^{6.5}$  at ambient temperatures. Upon cooling, changes in shear moduli at subzero temperatures are a rough two orders of magnitude in the glass transition region (from  $10^{6.5}$  to about  $10^{8.5}$  Pa). Furthermore, the predominant liquidlike response, which is the primary indication of glassy relaxation processes in model high sugar/biopolymer mixtures, is substantially diminished, and the trace of storage modulus dominates over that of loss modulus pushing the values of the damping factor ( $\tan \delta = G''/G'$ ) well below one (e.g.,  $\approx 0.53$  at  $-18$  °C in **Figure 3a**). At the lower range of temperatures, a hard solid response is obtained, which is known as the glassy state (34), with  $G'$  approaching constant

values (e.g.,  $10^{9.5}$  Pa at  $-57$  °C in **Figure 3b**) and those of  $G''$  diminishing rapidly.

**Correlation between Porosity Profile and Mechanical Glass Transition Temperature in Dehydrated Apple Tissue.** To circumvent the problem of a diminished glass transition in dehydrated apple tissue described in the preceding section and to identify an objective way to assess the temperature dependence of molecular processes in these systems, we decided to consider the following device: This entails plotting of the first derivative of shear modulus as a function of sample temperature vs the sample temperature for biomaterials that exhibit the classic rubber-to-glass transformation. The outcome is illustrated for the  $\kappa$ -carrageenan/sugar mixture in **Figure 2**. Interestingly, the derivative trace of storage modulus is reduced to a minimum at the conjunction of the WLF and modified Arrhenius equations, i.e., the very temperature spot leading to the fundamental derivation of the network  $T_g$ . Similar results have been reported for the structural properties of four distinct molecular weights of gelatin in the presence of cosolute (17), and as argued in the following section, it is hoped that the approach will be able to pinpoint vitrification phenomena in the dehydrated apple matrix.

The mechanical profile of such a system should be the outcome of a complex transformation occurring in a composite of low-mobility and amorphous segments. Drying of the apple tissue produces tightly packed domains of reduced molecular mobility (35), an outcome that according to the free volume theory diminishes the opportunity for a full manifestation of glassy phenomena in these systems. Synthetic polymer literature also provides evidence that increasing order in a material (i) enhances dramatically the rigidity of the rubbery region, (ii) reduces the viscous component of the network within the glass transition, and (iii) drops the value of the damping factor,  $\tan \delta$ , to well below one (36, 37). These are, indeed, the trademarks of the mechanical behavior of our materials depicted for the broad temperature range of 30 to  $-70$  °C in **Figure 3a–g**.

Furthermore, the essentials of partial vitrification in the amorphous phase of a composite system comprising an ordered or crystalline domain originate from the same molecular dynamics of chain segments in amorphous materials exhibiting a fully developed glass transition (38, 39). Building on that, we considered the storage-modulus derivative as the appropriate parameter for probing the fundamental manifestation of the mechanical  $T_g$  for apple tissue. This undertaking constitutes an effort to avoid utilization of empirical mechanical indicators [ $\tan \delta$  or  $G''$  maxima during vitrification or change in slope of the  $G'$  trace as a function of temperature (40)] in the derivation of a relationship between porosity and structural characteristics.

**Figure 3a–g** reproduces the application of this approach to several dehydrated apple disks with an apparent porosity range of 0.38–0.79. Data yield smooth first-derivative curves, with the relaxation spectrum of the viscous component of the network unraveling rapidly, as compared to the solid element for these preparations. This is also the case in the temperature profile of the loss modulus in **Figure 2**. The minimum of the storage modulus trace clearly demarcates the mechanical glass transition temperature, and it has been highlighted as a function of the volume fraction of total pores in **Figure 4**. Rheological studies for all systems exhibit a constant and negative gradient in the trend of the network  $T_g$  with increasing apparent porosity.

**Figure 4** also reproduces corresponding readings of the glass transition temperature obtained from DSC, a sample of which was given earlier in **Figure 1**. In contrast to rheology, the values of DSC  $T_g$  are independent of the level of porosity and remain fixed at  $-47.7 \pm 1$  °C. Furthermore, results suggest that under

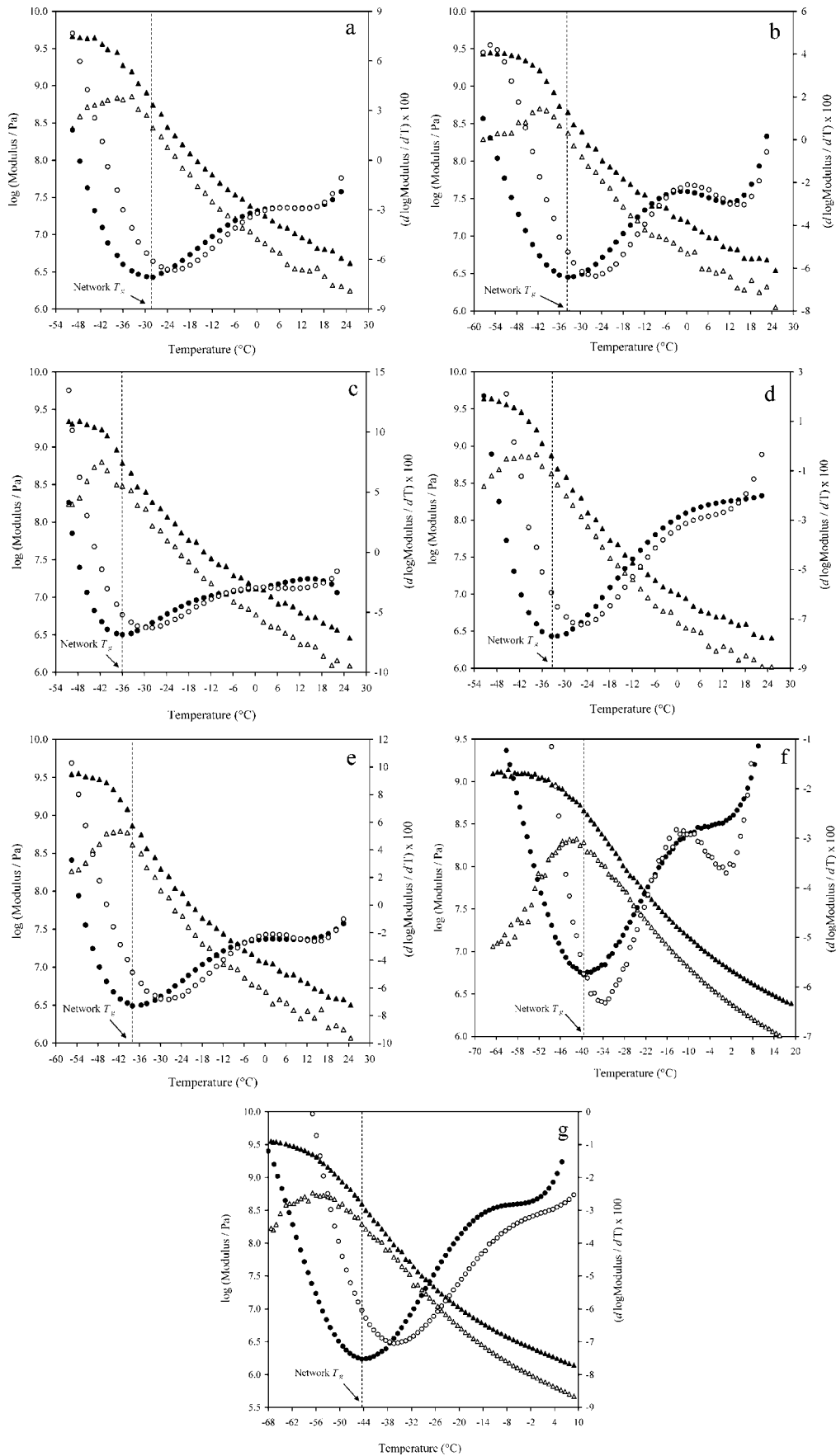


**Figure 3.** Cooling/heating profiles of storage ( $G'$ ;  $\blacktriangle$ ) and loss ( $G''$ ;  $\triangle$ ) modulus for dried apple at  $\approx 81\%$  solids (scan rate,  $1\text{ }^\circ\text{C}/\text{min}$ ; frequency,  $1\text{ rad/s}$ ; strain, 2 to  $0.00075\%$ ) (left y-axis) and first derivative plots of  $\log G'$  ( $\bullet$ ) and  $\log G''$  ( $\circ$ ) as a function of sample temperature plotted against temperature (right y-axis) with a total pore content of (a) 0.38, (b) 0.54, (c) 0.55, (d) 0.56, (e) 0.64, (f) 0.65, and (g) 0.79. The dashed line pinpoints the predictions of the mechanical  $T_g$ .

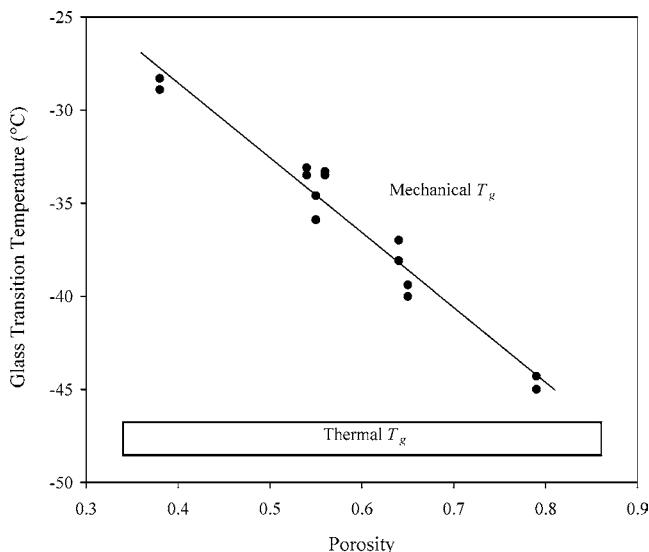


**Figure 4.** Variation of the mechanical and thermal glass transition temperature with increasing apparent porosity of the dehydrated apple tissue.

conditions of extremely high pore content both DSC and rheology should yield comparable estimates of the glass transition temperature.

To assist in the rationalization of the above findings, we employed scanning electron microscopy, which is a technique capable of providing tangible evidence of the transformation in the three-dimensional morphology with drying (41). **Figure 5a–c** illustrates such changes in the cellular organization in relation to the extrema and middle values of the experimentally accessible porosity in the apple matrix. It appears that at the lowest range of pore volume (0.38), drying caused the least destruction of the microstructure, with cells forming organized compartments that adhere to each other (**Figure 5a**). Increase in the severity of processing caused damage in cells, which appear to be open, flattened, and with a less cohesive continuous structure (porosity of 0.56 in **Figure 5b**). Finally, there is extensive damage of cell walls and loss of the highly organized tissue morphology at the upper range of porosity (0.79) in **Figure 5c**. This cellular collapse has created sizable voids (pores) among the remnants of the original continuous organization.

**Conclusion.** Analysis of the structural properties of the dehydrated apple tissue at constant moisture content but with distinct levels of porosity is greatly facilitated by combining calorimetry, rheology, and microscopy data and adopting a fundamental approach in the pinpointing of the mechanical glass transition temperature. Rheological estimates of  $T_g$  are strongly affected and diminish rapidly (from about  $-28.3$  to  $-45.0$  °C) with increasing pore volume (from 0.38 to 0.79), whereas the DSC counterparts exhibit a flat porosity dependence ( $T_g$  midpoint  $\approx -47.7$  °C). It is evidenced from the micrographs that prolonged processing and the creation of high levels of intercellular spaces lead to the disintegration of the apple matrix and the destruction of its continuity. The magnitude of the structural weakening is probed in the mechanical profile as a reduction in the values of the macromolecular glass transition temperature. Thus, the lower the volume fraction of total pores is, the more intact the cell walls and the greater the extent to which the mechanical  $T_g$  differs from the measurements of calorimetry. The latter appears to be insensitive to the macromolecular (network) morphology of the dried apple tissue.

Finally, the present work further supports an underlying

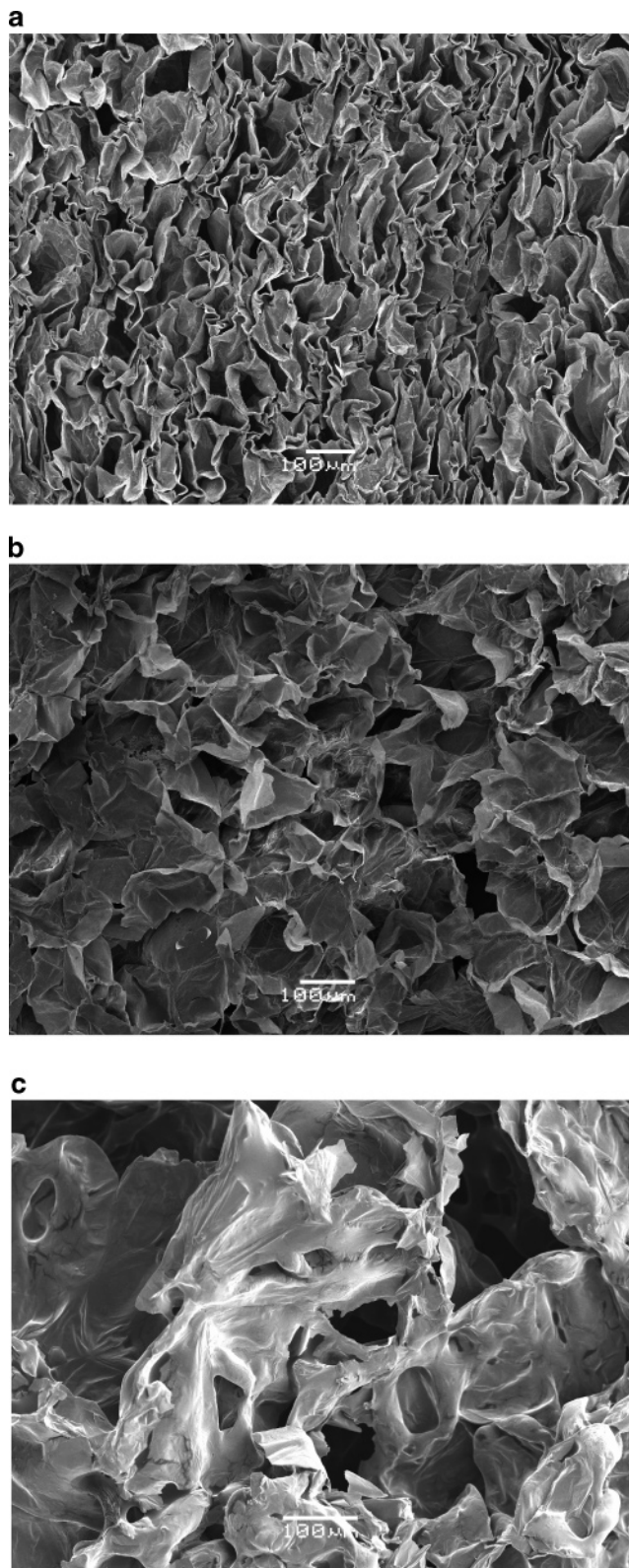


**Figure 5.** Micrographs of the interior microstructure of dehydrated apple tissue at apparent porosity levels of (a) 0.38, (b) 0.56, and (c) 0.79. Bar is 100  $\mu\text{m}$ .

process that becomes increasingly apparent in the literature. This relates to the observation that besides a thorough description of the material in terms of its composition or preparation history, the glass transition temperature depends on the analytical method and protocol employed (42–44). Thus, the discrepancies observed in the values of mechanical and DSC  $T_g$  in **Figure 4**

as a function of apparent porosity in apple tissue are not an experimental artifact but, rather, a reflection of the distinct property and distance scale being probed by the two techniques.

#### LITERATURE CITED

- (1) Parks, G. S.; Huffman, H. M. Glass as a fourth state of matter. *Science* **1926**, *LXIV*, 363–364.
- (2) Rahman, M. S. Glass transition and other structural changes in foods. *Handbook of Food Preservation*; Marcel Dekker: New York, 1999; pp 75–93.
- (3) Rahman, M. S. Phase transitions in foods. *Food Properties Handbook*; CRC Press: Boca Raton, FL, 1995; pp 87–177.
- (4) Slade, L.; Levine, H. Beyond water activity: Recent advances based on an alternative approach to the assessment of food quality and safety. In *Critical Reviews in Food Science and Nutrition*; Clydesdale, F. M., Ed.; CRC Press: Boca Raton, FL, 1991; Vol. 30 (2–3), pp 115–360.
- (5) White, G. W.; Cakebread, S. H. The glassy state in certain sugar-containing food products. *J. Food Technol.* **1966**, *1*, 73–82.
- (6) Roos, Y. H. Prediction of the physical state. *Phase Transitions in Foods*; Academic Press: San Diego, CA, 1995; pp 157–192.
- (7) Regand, A.; Goff, H. D. Structure and ice recrystallisation in frozen stabilized ice cream model systems. *Food Hydrocolloids* **2003**, *17*, 95–102.
- (8) Truong, V.; Bhandari, B. R.; Howes, T. Optimization of co-current spray drying process of sugar-rich foods. Part I—Moisture and glass transition temperature profile during drying. *J. Food Eng.* **2005**, *71*, 55–65.
- (9) Slade, L.; Franks, F. Appendix I: Summary report of the discussion symposium on chemistry and application technology of amorphous carbohydrates. In *Amorphous Food and Pharmaceutical Systems*; Levine, H., Ed.; The Royal Society of Chemistry: Cambridge, United Kingdom, 2002; pp x–xxvi.
- (10) Reid, D. S. Use, misuse and abuse of experimental approaches to studies of amorphous aqueous systems. In *Amorphous Food and Pharmaceutical Systems*; Levine, H., Ed.; The Royal Society of Chemistry: Cambridge, United Kingdom, 2002; pp 325–338.
- (11) Perry, P. A.; Donald, A. M. The effect of sugars on the gelatinisation of starch. *Carbohydr. Polym.* **2003**, *49*, 155–165.
- (12) Kumagai, H.; MacNaughtan, W.; Farhat, I. A.; Mitchell, J. R. The influence of carrageenan on molecular mobility in low moisture amorphous sugars. *Carbohydr. Polym.* **2002**, *48*, 341–349.
- (13) Roos, Y. H.; Karel, M. Applying state diagrams to food processing and development. *Food Technol.* **1991**, *45*, 66, 68–71, 107.
- (14) Roos, Y. H.; Karel, M.; Kokini, J. L. Glass transitions in low moisture and frozen foods: Effects on shelf life and quality. *Food Technol.* **1996**, *November*, 95–108.
- (15) Kasapis, S.; Al-Marhoobi, I. M.; Mitchell, J. R. Molecular weight effects on the glass transition of gelatin/co-solute mixtures. *Biopolymers* **2003**, *70*, 169–185.
- (16) Kasapis, S.; Al-Marhoobi, I. M. A.; Giannouli, P. Molecular order versus vitrification in high-sugar blends of gelatin and  $\kappa$ -carrageenan. *J. Agric. Food Chem.* **1999**, *47*, 4944–4949.
- (17) Kasapis, S. Definition and applications of the network glass transition temperature. *Food Hydrocolloids* **2006**, *20*, 218–228.
- (18) Bengtsson, G. B.; Rahman, M. S.; Stanley, R. A.; Perera, C. O. Apple rings as a model for fruit drying behavior: Effects of surfactant and reduced osmolality reveal biological mechanisms. *J. Food Sci.* **2003**, *68*, 563–570.
- (19) Mayor, L.; Sereno, A. M. Modelling shrinkage during convective drying of food materials: A review. *J. Food Eng.* **2004**, *61*, 373–386.
- (20) Akiyama, T.; Hayakawa, K. Heat and moisture transfer and hygrophysical changes in elastoplastic hollow cylinder-food during drying. *J. Food Sci.* **2000**, *65*, 315–323.
- (21) Le Bourvellec, C.; Renard, C. M. G. C. Non-covalent interaction between procyanidins and apple cell wall material. Part II: Quantification and impact of cell wall drying. *Biochim. Biophys. Acta* **2005**, *1725*, 1–9.
- (22) Sa, M. M.; Figueiredo, A. M.; Sereno, A. M. Glass transitions and state diagrams for fresh and processed apple. *Thermochim. Acta* **1999**, *329*, 31–38.
- (23) Krokida, M. K.; Karathanos, V. T.; Maroulis, Z. B. Effect of freeze-drying conditions on shrinkage and porosity of dehydrated agricultural products. *J. Food Eng.* **1998**, *35*, 369–380.
- (24) Rahman, M. S. A theoretical model to predict the formation of pores in foods during drying. *Int. J. Food Prop.* **2003**, *6*, 61–72.
- (25) Krokida, M. K.; Zogzas, N. P.; Maroulis, Z. B. Modelling shrinkage and porosity during vacuum dehydration. *Int. J. Food Sci. Technol.* **1997**, *32*, 445–458.
- (26) Walton, A. Modern rheology in characterizing the behaviour of foods. *Food Sci. Technol. Today* **2000**, *14*, 144–146.
- (27) Verdonck, E.; Schaap, K.; Thomas, L. C. A discussion of the principles and applications of modulated temperature DSC (MTDSC). *Int. J. Pharm.* **1999**, *192*, 3–20.
- (28) Stokke, B. T.; Elgsaeter, A. Conformation, order-disorder conformational transitions and gelation of non-crystalline polysaccharides using electron microscopy. *Micron* **1994**, *25*, 469–491.
- (29) Roos, Y. H. Effect of moisture on the thermal behaviour of strawberries studied using differential scanning calorimetry. *J. Food Sci.* **1987**, *52*, 146–149.
- (30) Mehl, P. M. Fictive glass-transition temperatures and fragility for the phase diagram of the system fructose/water. *Thermochim. Acta* **1998**, *324*, 215–221.
- (31) Ferry, J. D. Some reflections on the early development of polymer dynamics: Viscoelasticity, dielectric dispersion, and self-diffusion. *Macromolecules* **1991**, *24*, 5237–5245.
- (32) Ferry, J. D. Dependence of viscoelastic behavior on temperature and pressure. *Viscoelastic Properties of Polymers*; John Wiley: New York, 1980; pp 264–320.
- (33) Kasapis, S.; Al-Marhoobi, I. M.; Mitchell, J. R. Testing the validity of comparisons between the rheological and the calorimetric glass transition temperatures. *Carbohydr. Res.* **2003**, *338*, 787–794.
- (34) Padmanabhan, M. The application of rheological thermal analysis to foods. In *Proceedings of the 3rd International Symposium on Food Rheology and Structure*; Fischer, P., Marti, I., Windhab, E. J., Eds.; Laboratory of Food Process Engineering: ETH Zürich, Switzerland, 2003; pp 447–448.
- (35) Bai, Y.; Rahman, M. S.; Perera, C. O.; Smith, B.; Melton, L. D. Structural changes in apple rings during convection air-drying with controlled temperature and humidity. *J. Agric. Food Chem.* **2002**, *50*, 3179–3185.
- (36) Favier, V.; Chanzy, H.; Cavaillé, J. Y. Polymer nanocomposites reinforced by cellulose whiskers. *Macromolecules* **1995**, *28*, 6365–6367.
- (37) Ward, I. M.; Hadley, D. W. Experimental studies of linear viscoelastic behaviour as a function of frequency and temperature: Time-temperature equivalence. *An Introduction to the Mechanical Properties of Solid Polymers*; John Wiley & Sons: Chichester, United Kingdom, 1993; pp 84–108.
- (38) Montserrat, S.; Hutchinson, J. M. On the measurement of the width of the distribution of relaxation times in polymer glasses. *Polymer* **2002**, *43*, 351–355.
- (39) Kasapis, S. Definition of a mechanical glass transition temperature for dehydrated foods. *J. Agric. Food Chem.* **2004**, *52*, 2262–2268.
- (40) Ross, K. A.; Campanella, O. H.; Okos, M. R. The effect of porosity on glass transition measurement. *Int. J. Food Prop.* **2002**, *5*, 611–628.
- (41) Lewicki, P. P.; Porzecka-Pawlak, R. Effect of osmotic dewatering on apple tissue structure. *J. Food Eng.* **2005**, *66*, 43–50.

- (42) Schmidt, S. J. Probing the physical and sensory properties of food systems using NMR spectroscopy. In *Advances in Magnetic Resonance in Food Science*; Belton, P. S., Hills, B. P., Webb, G. A., Eds.; The Royal Society of Chemistry: Cambridge, United Kingdom, 1999.
- (43) Schmidt, S. J. Water and solids mobility in foods. *Adv. Food Nutr. Res.* **2004**, *48*, 1–101.
- (44) Kasapis, S.; Mitchell, J.; Abeysekera, R.; MacNaughtan, W. Rubber-to-glass transitions in high sugar/biopolymer mixtures. *Trends Food Sci. Technol.* **2004**, *15*, 298–304.

---

Received for review December 1, 2006. Accepted January 24, 2007.

JF063473J